IOPscience iopscience.iop.org

Home Search Collections Journals About Contact us My IOPscience

Extended x-ray absorption fine structure study of the MnAs local structure at the phase transitions

This article has been downloaded from IOPscience. Please scroll down to see the full text article.

2005 J. Phys.: Condens. Matter 17 1537

(http://iopscience.iop.org/0953-8984/17/10/009)

View the table of contents for this issue, or go to the journal homepage for more

Download details:
IP Address: 129.252.86.83
The article was downloaded on 27/05/2010 at 20:25

Please note that terms and conditions apply.

INSTITUTE OF PHYSICS PUBLISHING JOURNAL OF PHYSICS: CONDENSED MATTER

J. Phys.: Condens. Matter **17** (2005) 1537–1545 doi:10.1088/0953-8984/17/10/009

Extended x-ray absorption fine structure study of the MnAs local structure at the phase transitions

O Palumbo[1], **C Castellano, A Paolone and R Cantelli**

Università di Roma 'La Sapienza', Dipartimento di Fisica, Piazzale Aldo Moro 2, I-00185, Roma, Italy
and
INFM, Italy

E-mail: oriele.palumbo@roma1.infn.it

Received 26 July 2004, in final form 23 December 2004
Published 25 February 2005
Online at stacks.iop.org/JPhysCM/17/1537

Abstract

Extended x-ray absorption fine structure measurements at the Mn K absorption edge on MnAs in the temperature range between 250 and 500 K are reported. The temperature dependence of the interatomic Mn–Mn and Mn–As distances is in accordance with the lattice parameter behaviour reported by previous diffraction studies. The Debye–Waller factors of the Mn–Mn and Mn–As first sub-shells are both characterized by an anomaly near the first-order magnetostructural transition at T_C. This critical behaviour is superimposed on a temperature dependence well described by a correlated Debye model and is analysed in terms of a cusp-shaped anomaly strictly related to a critical lowering in the phonon frequencies.

1. Introduction

Manganese monoarsenide (MnAs) is a ferromagnetic compound extensively studied during the last century, which has recently received new attention since it shows properties potentially important for a variety of magnetic [1] and magnetoelectronic [2] applications. Moreover, great interest in this compound arose again as a consequence of the analogies between its behaviour and that of the manganese oxide perovskites [3, 4]. MnAs is ferromagnetic with hexagonal NiAs-type structure ($B8_1$) at low temperature and transforms, at about $T_C \simeq 313$ K, into a paramagnetic phase with a distorted orthorhombic MnP-type structure ($B31$). This transformation is a first-order magnetostructural phase transition accompanied by a discontinuous increase of the molar volume (about 2%) and by a decrease of the electrical conductivity revealing a metal–insulator transition [5, 6]. On heating, at about $T_t = 399$ K, a second-order structural phase transition with no volume change occurs: the orthorhombic distortion decreases with increasing temperature and the hexagonal ($B8_1$)

[1] Author to whom any correspondence should be addressed.

structure reappears above T_t [7]. Indeed, both transitions and the anomalous behaviour of the magnetic susceptibility in the intermediate phase have been explained by Goodenough [8–10] assuming a change of the Mn spin state, from a high spin state in the $B8_1$ phase to a low spin state in the $B31$ phase. The spin state instability appears to be responsible for a giant magnetoelastic response recently reported [11] and is also emphasized by an attempted explanation of the magnetic properties and of the magnetovolume effects in MnAs from the viewpoint of itinerant electrons [12].

Recently, neutron diffraction experiments [3] showed that an external magnetic field B stabilizes the hexagonal phase above T_C. The field-induced phase transition is accompanied by an enhanced magnetoresistance of about 17% at 310 K. This phenomenon seems to have the same origin as that observed in the manganites, even if the absolute value is not as large as in compounds like $La_{1-x}Ca_xMnO_3$ with $0.2 < x < 0.5$. Similarities between MnAs and colossal magnetoresistance (CMR) manganites have been found also in the local structure behaviour. In fact, EXAFS measurements on MnAs [4] at the Mn K edge in the temperature range between 10 and 300 K show that the total disorder and the static contribution to the disorder in the basal Mn–As plane are greater than along the apical Mn–Mn direction. In particular, the static contribution to the local disorder in the Mn–As shell is comparable to the one found in $LaMnO_3$ manganites [13] and attributed to the Jahn–Teller distortion of the MnO_6 octahedra, which contributes to the CMR. These similarities have suggested that in MnAs the great disorder in the basal plane could be due to a local lattice distortion [4]. The results obtained for the local structure below T_C agree with the suggested [3, 14] key role of the local lattice distortion in the magnetic and structural MnAs properties. The present work extends the previously reported low temperature EXAFS measurements to the temperature range between 250 and 500 K, allowing the study of the local structure in the paramagnetic phase. Moreover, this study supplies information about the local lattice disorder and its characteristic behaviour near the two phase transitions. These measurements also highlight the analogy between MnAs and systems with large static disorder like manganites, characterized by a strong electron–phonon coupling but also by a relevant magnetic component in charge localization.

2. Experimental method and data analysis

The samples studied were pellets of polycrystalline commercial MnAs powder, provided by Great Western Inorganics, dissolved in a graphite matrix. Mn K-edge EXAFS data were recorded in transmission geometry at the beamline BM29 at the European Synchrotron Radiation Facility (ESRF-Grenoble). Measurements were performed on heating at various temperatures between 250 and 500 K, using a helium flux cryostat below room temperature and a heater connected to a graphite holder in the temperature range between 290 and 500 K. The k weighted EXAFS oscillations ($k\chi(k)$) were extracted from the experimental data using standard procedures [15] and were normalized using the Lengeler–Eisenberger [16] method, with $E_0 = 6539$ eV. Some examples of the data obtained are shown as a function of the temperature in figure 1(a); the essential structural features are well reproducible over the whole temperature range. The k^3 weighted $\chi(k)$ data were Fourier transformed (FFT) in the k range between 3.46 and 13.88 $Å^{-1}$. The Fourier transform obtained shows many correlation peaks up to $R = 7$ Å, as expected for an ordered crystalline structure. A typical FFT signal is reported in figure 1(b). The analysis was restricted to the first-shell FFT peak, corresponding to the superposition of the Mn–As and Mn–Mn neighbour contributions, by inverse Fourier transforming (Fourier filtering) the data in the R range 1.53–2.64 Å. The filtered data were fitted using the standard single-scattering EXAFS formula and theoretical amplitude and phase functions [17].

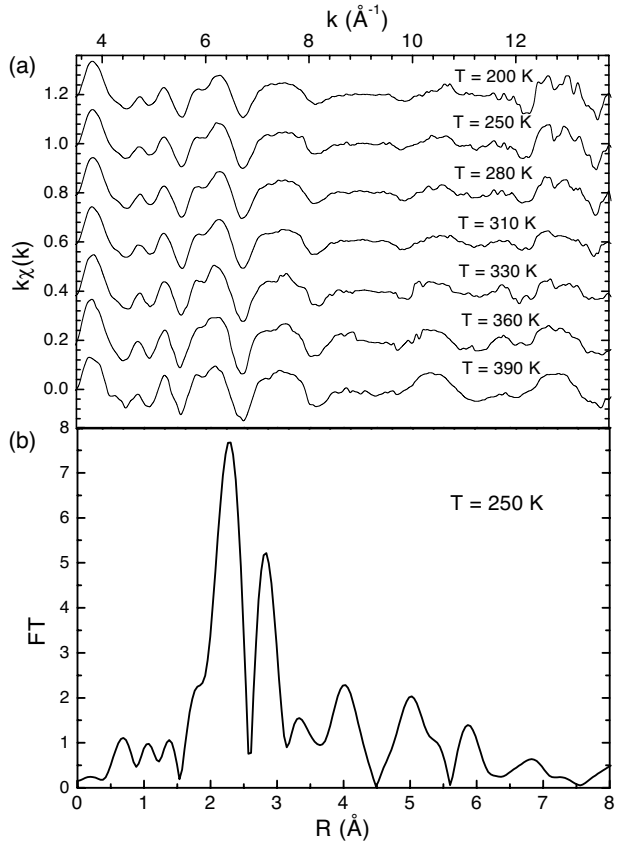

Figure 1. (a) k weighted EXAFS signals as a function of the temperature between 200 K (upper curve) and 390 K (lower curve); (b) a typical FT signal for the MnAs sample in the ferromagnetic state at 250 K.

The data taken below T_C and above T_t, namely with the sample in the hexagonal $B8_1$ phase, have been analysed using the model previously reported [4] to describe the low temperature ferromagnetic phase. In this model two sub-shells were required to fit the data: one corresponding to the $N_{Mn-As} = 6$ As atoms in the hexagonal unit cell and the other corresponding to the $N_{Mn-Mn} = 2$ out-of-plane Mn atoms. The two sub-shells fit was possible due to the extension of the data in the k range, to the windowing in the FFT space, to the number of independent fitting parameters and to the good signal to noise ratio. During the fitting process, the coordination numbers N_{Mn-Mn} and N_{Mn-As} were fixed to the previous reported values, according to other EXAFS experiments performed at fixed temperature [18]. In this way the uncertainty on the mean square relative displacements of the bond lengths (or Debye–Waller factor), σ^2, was reduced. The fitting parameters were σ^2_{Mn-As}, σ^2_{Mn-Mn} and the interatomic bond lengths for the two sub-shells. The interatomic distances used as starting points for the fit were the values obtained from crystallographic parameters [18, 19], i.e. $R_{Mn-As} = 2.75$ Å and $R_{Mn-Mn} = 2.65$ Å.

The distorted orthorhombic $B31$ structure is derived from the $B8_1$ phase by a cooperative displacement of pair of $[1, \bar{1}, 0]$ rows toward one another [3]. In the $B8_1$ phase each Mn atom is surrounded by two Mn atoms and six As atoms at the same distance; in contrast, in

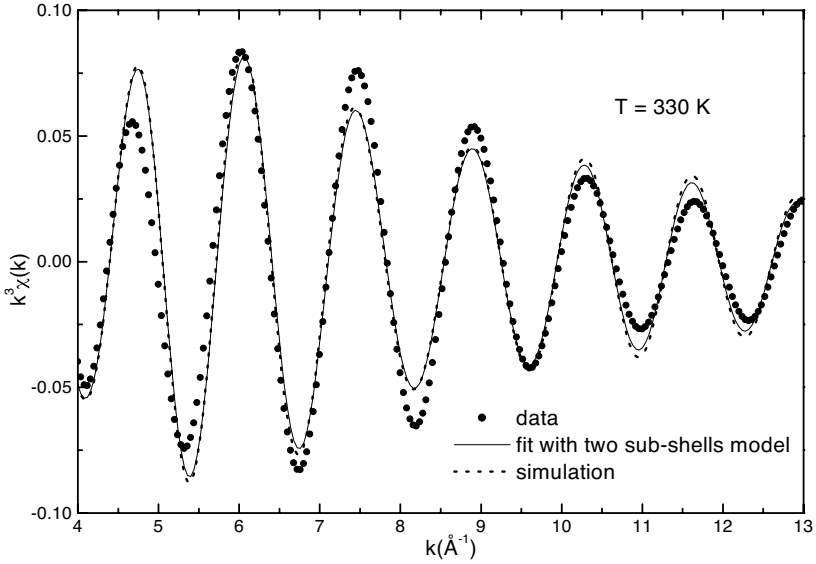

Figure 2. The FFT XAFS signal at $T = 330$ K (symbols), the best fit curve considering the two-sub-shell model (solid curve) and the simulation based on the orthorhombic distorted crystallographic structure.

the distorted orthorhombic phase, the Mn–As distances are split [20]. To be precise, x-ray diffraction measurements [21] showed that in the orthorhombic phase there are two different Mn–As distances along [001] whilst the other four Mn–As bonds are not significantly different from each other or from the Mn–As distance in the $B8_1$ phase just below T_C. The difference among the six Mn–As distances is very slight (<3.5% from data in [21]) and is not well describable in the framework of the reported measurements. In fact due to the extension of the data in the k range and to the great number of independent fitting parameters required it is not possible to carry out a multi-shell analysis taking into account both the Mn–Mn shell and the three Mn–As sub-shells, namely one for each distance originated from the orthorhombic distortion. Therefore the model with only two sub-shells, one corresponding to $N_{\mathrm{Mn-As}} = 6$ As atoms and the other corresponding to the $N_{\mathrm{Mn-Mn}} = 2$ apical Mn atoms, has been used also for the analysis in the orthorhombic phase. For comparison, in figure 2 a typical fit with two sub-shells in the paramagnetic phase is presented together with a simulation of the FFT XAFS signals based on the orthorhombic distorted crystallographic structure. The very little differences between the best fit and the simulation curves allow the use of the two-sub-shell model in our approach. The fitting procedure is the same as that described just above for the $B8_1$ phase.

3. Results

The temperature dependences of the interatomic distances ($R_{\mathrm{Mn-As}}$ and $R_{\mathrm{Mn-Mn}}$) and of the Debye–Waller factors for the two bond lengths ($\sigma^2_{\mathrm{Mn-As}}$ and $\sigma^2_{\mathrm{Mn-Mn}}$) are respectively plotted in figures 3 and 4.

Below T_C, the present results are in good agreement with those obtained from previous EXAFS measurements [4] between 10 and 300 K, as shown in figure 3 where present results are shown together with data points from previous work. Despite the fact that the uncertainties on the distances are of the order of 0.01 Å, i.e. comparable with the excursion of the data,

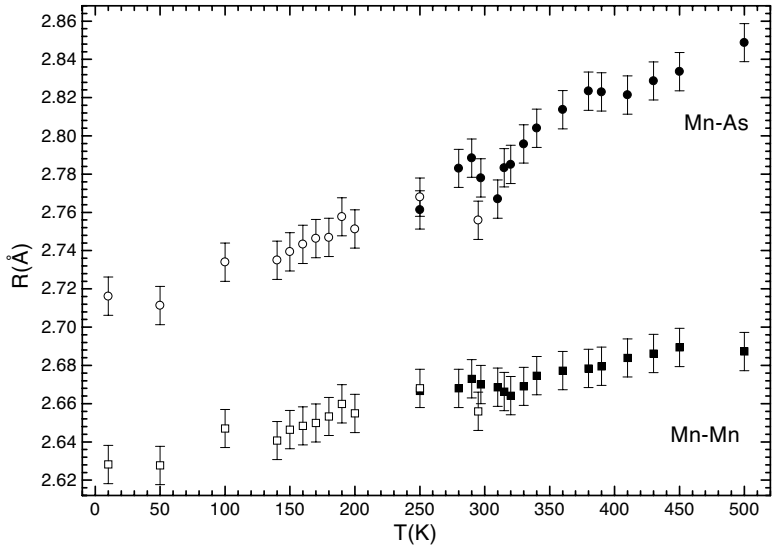

Figure 3. Mn–Mn (squares) and Mn–As (dots) bond lengths as a function of temperature. Full symbols refer to the present work, open symbols to the previous one [4].

some information can be obtained from the trend of the mean distance as a function of the temperature. Figure 3 shows that below room temperature both interatomic distances decrease, in agreement with the unit cell contraction reported from x-ray diffraction experiments in the temperature range from room temperature down to 100 K [7]. Above the Curie temperature ($T_C \simeq 313$ K), instead, the two distances increase with temperature, showing a behaviour in agreement with the temperature dependence of the lattice parameters [7]. Both Mn–Mn and Mn–As distances have a dip in their trend near the magnetic transition, recalling the discontinuous decrease of the molar volume behaviour. However, a possible influence on this feature of a harmonic approximation choice for the fluctuation regime cannot be ruled out.

In figure 4 the Debye–Waller factors of the two bond lengths, $\sigma^2_{\mathrm{Mn-As}}$ and $\sigma^2_{\mathrm{Mn-Mn}}$, show the same trend, even if their absolute values indicate that the Mn–Mn sub-shell is less disordered than the Mn–As one. As references, $\sigma^2_{\mathrm{Mn-As}}$ and $\sigma^2_{\mathrm{Mn-Mn}}$ from previous work on the ferromagnetic phase are reported in figure 4. These data show qualitative agreement with the present data as regards behaviour, except for the high $\sigma^2_{\mathrm{Mn-Mn}}$ value obtained at 250 K in previous work. The values of $\sigma^2_{\mathrm{Mn-As}}$ and $\sigma^2_{\mathrm{Mn-Mn}}$ are both characterized by a cusp-shaped anomaly near T_C. This anomaly is superimposed on the 'usual' Debye–Waller factor temperature dependence.

These features can be described considering that σ^2 is composed of three terms, namely a temperature independent static contribution, σ^2_S, and two temperature dependent dynamic contributions: σ^2_D, which accounts for the ordinary increase of σ^2 with the temperature, and σ^2_T, which accounts for the critical behaviour in the neighbourhood of the first-order phase transitions. In the Debye approximation, σ^2_D can be expressed as an infinite series whose first terms are [22]

$$\sigma^2_D = \frac{3\hbar^2}{Mk_B\theta_D}\left[\frac{1}{4} + \left(\frac{T}{\theta_D}\right)^2 \int_0^{\frac{\vartheta_D}{T}} \mathrm{d}x \frac{x}{\mathrm{e}^x - 1}\right] \tag{1}$$

where M is the mass of the diffusing atom and θ_D is the Debye temperature. The above formula shows that, once the mass of the atoms is known, σ^2_D is a function of the Debye temperature

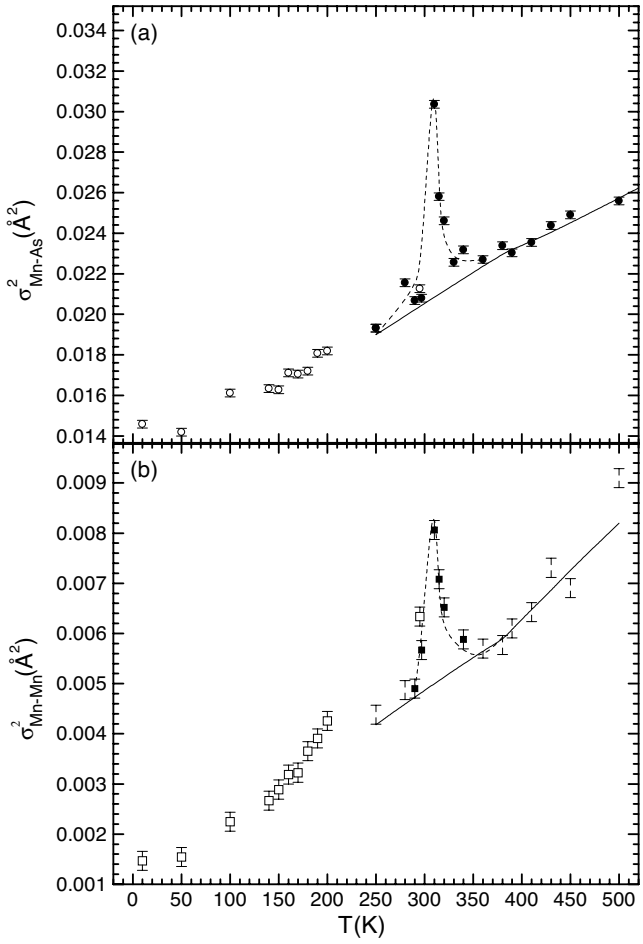

Figure 4. Debye–Waller factors for Mn–As (a) and Mn–Mn (b) sub-shells. Full symbols refer to the present work, open symbols to the previous one [4]. The curves are best fit contributions: thermal (solid curve) and critical (dashed curve). The static contributions to the local disorder obtained are: for the Mn–Mn sub-shell $\sigma^2_S = 0.002\,05$ Å^2 and for the Mn–As sub-shell $\sigma^2_S = 0.011\,33$ Å^2.

alone. The anomalous critical dependence of σ^2 near a displacive first-order phase transition is described with the approximate expression [23, 24]

$$\sigma^2_T \propto \frac{T}{(T - T_O)^\gamma} \tag{2}$$

where T_O is the temperature at which the crystal would become unstable (not necessarily $T_O = T_C$ [24]) and γ is a critical exponent derived from the dispersion relation of the phonon frequencies.

Both the Mn–Mn and Mn–As Debye–Waller factors have been successfully fitted considering $\sigma^2(T) = \sigma^2_D + \sigma^2_S + \sigma^2_T$. The fitting parameters were the static contribution to the local disorder σ^2_S, the Debye temperature θ_D, the critical temperature T_O and the exponent γ. The different contributions to the best $\sigma^2(T)$ fit curve obtained, namely the static, the thermal and the critical dependences, are shown in figure 4. The Debye temperature was found to be 310 K, in agreement with the literature data [25]. The static contribution to the

local disorder obtained confirms that the Mn–Mn sub-shell ($\sigma_S^2 = 0.002\,05$ Å^2) is much less statically disordered than the Mn–As sub-shell ($\sigma_S^2 = 0.011\,33$ Å^2): above room temperature both the total disorder and the static contribution to the disorder in the Mn–As sub-shell are greater than that along the apical Mn–Mn direction, in agreement with our previous results [4]. The value for the temperature T_O was found to be 311 K, which is, within the experimental error, very close to T_C, and the critical indices obtained for the two shells $\gamma_{Mn-As} = 0.5167$ and $\gamma_{Mn-Mn} = 0.4462$ are slightly different.

4. Discussion

The Debye–Waller factor (DWF), provided by Mössbauer fraction, x-ray and neutron experiments, is one of the most important parameters in describing the phase transition in terms of local structure. EXAFS provides the correlated Debye–Waller factor for a certain pair of atoms (absorber and backscatterer), which could describe the phase transition appropriately. Several EXAFS works have been reported that examined DWF temperature behaviour in phase transitions: for example the melting transition of Pb showed no definite anomaly of the DWF at the melting point, while the anomaly of the DWF in high T_C superconductors is still under discussion [26]. Moreover in manganites a sudden decrease of the DWF near T_C indicates progressive reduction of charge–lattice coupling through the metal–insulator phase transition [27]. An anomalous temperature dependence of the DWF has indeed been reported also for ferroelectrics like $BaTiO_3$ and $PbTiO_3$ [28] and the stoichiometric compound $Ge_xSn_{1-x}Te$ [23, 29].

X-ray diffraction study of MnAs single crystals [30] shows that there are no significant anomalies in the static displacements of the atoms as a result of the phase transitions at T_C and T_t. On the other hand, there are anomalous changes in the lattice dynamics at the critical temperature: the mean square displacements of atoms in the lattice start to increase below room temperature and reach their maximum values at the magnetic transition temperature T_C; then they decrease smoothly down to T_t and above T_t show the usual thermal rise. Those dynamic changes are connected to the lattice 'softening' on approaching T_C and to the lattice 'hardening' on further increasing of the temperature up to T_t. The temperature behaviour of the mean square displacements of atoms reported by the above x-ray diffraction study agrees with the σ^2 cusp-shaped anomaly reported in the present work.

Diffraction and EXAFS Debye–Waller factors present some differences, as the atomic DWF given by diffraction represents the mean square deviation of a given atom from its average site in the crystal, while the EXAFS Debye–Waller factor is expected to be derived from correlated motions of atoms, and the correlation gets reduced with disorder in the material [31]. The close similarities between diffraction and EXAFS data and the fundamental role of the lattice disorder in the magnetic and structural MnAs properties rule out any great influence of the correlation on the reported σ^2 cusp-shaped anomaly. This critical behaviour has been described with an approximate expression for σ_t^2 used in a Mössbauer study of the phase transition of $Ge_xSn_{1-x}Te$ [23] for the critical part of the recoilless fraction associated with the 'ferroelectric branch'. This approximation was obtained assuming an Ornstein–Zernike expression for the Fourier transform of the displacement correlation function [24] and has been explained theoretically on the assumption of a critical lowering in the phonon frequencies. Several works predicted a divergent mean square displacement at T_C using the Einstein oscillator approximation for the soft optical phonon mode [32] or the Debye model in connection with the vanishing shear modulus [33], but the anomalous behaviour of the DWF at T_C usually results from a critical behaviour of some specific phonon branches [34]. To our knowledge, for MnAs a dispersion relation of phonon modes has not been reported, but the

drop in the elastic modulus reduction and the maximum in the sound attenuation measured near the two transitions have been explained in terms of a phonon instability [35, 36], with a soft phonon frequency which goes to zero. The presence of this phonon instability justifies the use of the approximate expression (2) to describe the cusp near the first-order transition; on the other hand due to lack of knowledge of any temperature dependence for the phonon anomaly, the critical exponent γ has been considered as a fitting parameter.

Near the second-order structural transition temperature T_t no critical effect in the σ^2 behaviour has been observed, in agreement with the diffraction data [30], even if the existence of a soft phonon mode has been reported [35]. It was suggested [24] that the size of the critical increase near a transition is smaller for crystals in which the difference between the transition temperature and the temperature T_O is bigger, in agreement with (2), where T_O is not necessarily the transition temperature. This argument suggests that the anomaly near T_t exists but is too small to be detected on the Debye-like background.

5. Conclusion

The EXAFS spectrum of MnAs has been measured between 250 and 500 K. The temperature dependences of the interatomic Mn–Mn and Mn–As distances are in agreement with the temperature dependence of the lattice parameters. Moreover from the Debye–Waller factor of the two bond lengths, σ^2_{Mn-As} and σ^2_{Mn-Mn}, two types of information have been obtained. The first is the 'usual' temperature dependence, well described by the Debye approximation, and the second is the critical behaviour near the first-order phase transition, analysed in terms of a cusp-shaped anomaly strictly related to a critical lowering in the phonon frequencies.

Acknowledgments

The authors are grateful to Professor A Rigamonti for useful discussions and suggestions. This work was realized at the European Synchrotron Radiation Facility and we wish to thank S De Panfilis for assistance in using beamline BM29.

References

[1] Lane P, Cockaine B, Wright P J, Oliver P E, Tilsley M E G, Smith N A and Harris I 1994 *J. Cryst. Growth* **143** 237
[2] De Boeck J, Oesterholt R, Bender H, Van Esch A, Bruynseraede C, Van Hoof C and Borghs G 1996 *J. Magn. Magn. Mater.* **156** 148
[3] Mira J, Rivadulla F, Rivas J, Fondado A, Guidi T, Caciuffo R, Carsughi F, Radaelli P G and Goodenough J B 2003 *Phys. Rev. Lett.* **90** 097203
[4] Castellano C, Palumbo O, Paolone A and Cantelli R 2003 *Solid State Commun.* **125** 607
[5] Serres A 1947 *J. Phys. Radium* **8** 146
[6] Guillaud C 1951 *J. Phys. Radium* **12** 223
[7] Suzuki T and Ido H 1982 *J. Phys. Soc. Japan* **51** 3149
[8] Goodenough J B, Ridley D H and Newman W A 1964 *Proc. Int. Conf. on Magnetism (Nottingham)* (London: Inst. Phys. and Phys. Soc) p 542
[9] Goodenough J B and Kafalas J A 1967 *Phys. Rev.* **157** 389
[10] Menyuk N, Kafalas J A, Dwight K and Goodenough J B 1969 *Phys. Rev.* **17** 942
[11] Cherenko V A, Wee L, McCormick P G and Street R 1999 *J. Appl. Phys.* **85** 7833
[12] Motizuki K 1987 *J. Magn. Magn. Mater.* **70** 1
[13] Meneghini C, Castellano C, Kumar A, Ray S, Sarma D D and Mobilio S 1999 *Phys. Status Solidi* b **215** 647
[14] Govor G A 1985 *Phys. Status Solidi* a **90** K185
[15] Lee P A, Citrin P H, Eisenberger P and Kinkaid B M 1981 *Rev. Mod. Phys.* **53** 769
[16] Lengeler B and Eisenberger P 1980 *Phys. Rev.* B **21** 4507

[17] McKale A G 1988 *J. Am. Chem. Soc.* **110** 3763
[18] Huang S, Ming Z H, Soo Y L, Kao Y H, Tanaka M and Munekata H 1996 *J. Appl. Phys.* **79** 1435
[19] Willis B T and Rooksby H P 1954 *Proc. Phys. Soc.* B **67** 290
[20] Fjellvag H and Andresen A F 1984 *J. Magn. Magn. Mater.* **46** 29
[21] Wilson R H and Kasper J S 1964 *Acta Crystallogr.* **17** 95
[22] Beni G and Platzman P M 1976 *Phys. Rev.* B **14** 1514
[23] Rigamonti A and Petrini G 1970 *Phys. Status Solidi* **41** 591
[24] Borsa F and Rigamonti A 1972 *Phys. Lett.* A **40** 399
[25] Grønvold F, Snildal S and Westrum E F 1970 *Acta Chem. Scand.* **24** 285
[26] Yokoyama T, Murakami Y, Kiguchi M, Komatsu T and Kojima N 1998 *Phys. Rev.* B **58** 14238
[27] Booth C H, Bridges F, Kwei G H, Lawrence J M, Cornelius A L and Neumeier J J 1998 *Phys. Rev.* B **57** 10440
[28] Bhide V G and Hedge M S 1972 *Phys. Rev.* B **5** 3488
[29] Fano V, Fedeli G and Ortalli I 1977 *Solid State Commun.* **22** 467
[30] Govor G A 1981 *Sov. Phys.—Solid State* **23** 841
[31] Lanzara A, Saini N L, Bianconi A, Duc F and Bordet P 1999 *Phys. Rev.* B **59** 3851
[32] Cochran W 1960 *Adv. Phys.* **9** 387
[33] Schuster H and Bostock J 1971 *Phys. Lett.* A **35** 31
[34] Meissner G and Binder K 1975 *Phys. Rev.* B **12** 3948
[35] Bärner K and Berg H 1978 *Phys. Status Solidi* a **49** 545
[36] Ihlemann J and Bärner K 1984 *J. Magn. Magn. Mater.* **46** 40